

Polarization-sensitive absorber based on metamaterials

Zheng Zhu, Ruiqiang Zhao, Wenjin Lv, Jigang Bing, Yuxiang Li, Jinhui Shi*,

Key Laboratory of In-Fiber Integrated Optics of Ministry of Education
College of Science, Harbin Engineering University, Harbin 150001, China
E-mail: shijinhui@hrbeu.edu.cn

Abstract— We experimentally demonstrate polarization-sensitive coherent perfect absorption based on interaction between bilayered asymmetrically split rings (ASRs) metamaterial and a standing wave formed by two coherent counter propagating beams. The coherently controlled metamaterials provide an opportunity to realize selective-excited multiband absorption and ultrafast information processing.

Keywords—metamaterial; coherent perfect absorber; polarization

I. INTRODUCTION

Recent years metamaterials has been developing increasingly. Due to their unique geometries, metamaterials can control properties of electromagnetic wave to realize desirable amplitude, phase-shift or polarization conversion in unconventional way that can be unachievable using traditional materials [1-4]. As a special example of controlling amplitude of electromagnetic waves, metamaterial-based absorbers (MBA) can realize weak radiation and nearly total absorption [4]. The multiband, polarization-insensitive and angle-independent absorbers have been demonstrated from microwave, THz to optical range [4-6], etc. The coherent perfect absorption (CPA) is a kind of newly invented MBAs [7-9]. In metamaterials, the electric and magnetic resonances can be independently switched off/on by changing the phase difference between two coherent beams. The interaction between the metamaterial and standing wave realizes coherent perfect absorption [10-14], selective mode excitation [15, 16], coherent control of optical activity and optical anisotropy [17], coherent control of the gradient metasurface [18-22] and optical computation [23-25]. Therefore, coherent technique plays an important role in controlling electromagnetic transmission or other properties in the field of metamaterials, and it is necessary to study coherent interaction of a bilayered metamaterial with a standing wave.

II. METAMATERIAL DESIGN

In this work, we realize coherent perfect absorption (CPA) by the interaction between the standing wave and the bilayered metamaterial. As described earlier, if a metamaterial of subwavelength thickness is placed at a node or antinode of the standing wave, it will lead to different results in controlling intensity and absorption of the output beams [10] when two

coherent beams named “Signal Beam ” and “Coherent Beam ” pass though it normally shown in Fig. 1(a).

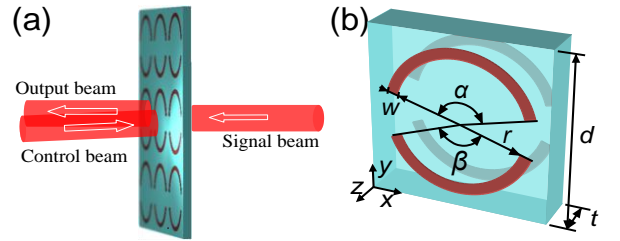


Fig. 1. The principle of coherent perfect absorption and snapshots of unit cells of bilayered metamaterials consisting of asymmetrically split rings (ASRs).

Generally, the nodes and antinodes of the standing wave are defined in the electric field. An electric antinode corresponds to the magnetic node, or vice versa. Firstly, if the ultrathin film is placed on electric nodes (corresponding to the phase difference of $\varphi = 180^\circ$ between two input beams), the metamaterial is transparent to both counter-propagating incident beams. In this case, the ASRs experiences no electric excitation, however, strong magnetic excitation in ASRs is twice larger than the case of one beam illumination. Secondly, two output beams totally vanish when the film is placed at an antinode (corresponding to the phase difference of $\varphi = 180^\circ$ between two input beams). In this case, twice electric excitation of the ASRs compared to one beam illumination and no magnetic excitation happen. When modulating phase of the coherent beam, the intensity of the output beam changes correspondingly. Here, the structures of bilayered asymmetrically split rings (ASRs) referred to Ref. 15 are shown in Fig. 1(b). The ASRs are periodic along the x and y directions with a lattice constant of $d = 15\text{mm}$. The ASRs etched from the copper cladding can be fabricated on either side of the FR4 printed circuit board with a thickness $t = 1.5\text{mm}$. Each ASR consists of two copper wire arcs with open angles of $\alpha = 140^\circ$ and $\beta = 160^\circ$. The inner radius of the ASRs is $r = 5.6\text{mm}$ and the wire width is $w = 0.8\text{mm}$. Each stereo ASR dimer consists of two spatially separated ASRs, which are structurally identical.

III. RESULTS AND DISCUSSIONS

Based on full-wave simulations using a three-dimensional Maxwell finite element method solver, the absorption spectra are shown in Fig. 2. In the simulations, the copper was treated

as a perfect electric conductor and a permittivity $\varepsilon = 4.05 - i0.05$ was assumed for the lossy dielectric substrate. The bilayered metamaterial exhibits triple-band absorption in the frequency range from 4 GHz to 8 GHz for an x-polarized input beams illumination while it exhibits double-band absorption in the frequency range from 8 GHz to 12 GHz for an y-polarized input beams illumination along the z direction, respectively. The both input beams are x- or y-polarized in the coherent case. The intensity of the beam is defined as 1 in the case of one beam illumination while the intensities of two input beams are defined as 0.5 in the coherent case. Obviously, the bilayered metamaterial reveals distinct absorption peaks at electric nodes and anti-nodes of the standing wave. More importantly, three absorption bands can be selectively switched on/off at lower frequencies and other two absorption bands occur at higher frequencies, depending on the phase difference of two input beams. Figure 2 shows the absorption spectra surface current density of the bilayered metamaterial. In Figure 2 (a) and (b), electric and magnetic responses can be selectively enhanced or eliminated with the phase difference varies for same polarization of input beams. It is clearly seen in Figure. 2 (c) and (d) that the coherent control by the second beam makes the bilayered metamaterial totally absorb all intensities of two input beams instead of half absorption in the single beam illumination.

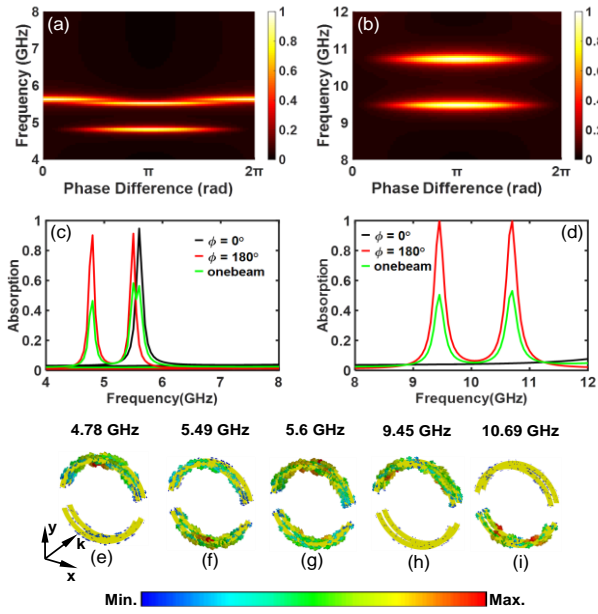


Fig. 2. Absorption spectra and surface current density of the bilayered metamaterial.

The coupling effects in stereometamaterial lead to the mode hybridization and thus multiple electric and magnetic resonances. In Figure 2(e)-(i), it shows surface current density of five resonances frequencies from lower (4.78 GHz, 5.49 GHz, 5.6 GHz when x-polarization incident) to higher (9.45 GHz, 10.69 GHz when y-polarization incident). More importantly, five absorption bands can be selectively switched on/off, depending on the phase difference of two input beams.

In figures. 2(a) and 2(b), it reveals a peak at 5.6 GHz with absorption of 94.7% when the phase difference is $\varphi = 0^\circ$; however, as $\varphi = 180^\circ$, this absorption peak is switched off and two other peaks appear at 4.86 GHz with x-polarization incident. Similarly, this coherent switching effect is found when incident wave is y-polarization. Two peaks at 9.45 GHz and 10.7 GHz with absorption of 99.9% and 99.7% occur for $\varphi = 180^\circ$, respectively. However, the two peaks in Fig. 2(c) are too close to recognize from each other easily when one beam illumination. In Fig. 2(a), it shows the different resonant modes, two absorption peaks can be totally separated at different phase difference. Obviously, the bilayered metamaterial reveal distinct absorption peaks at electric nodes and anti-nodes of the standing wave.

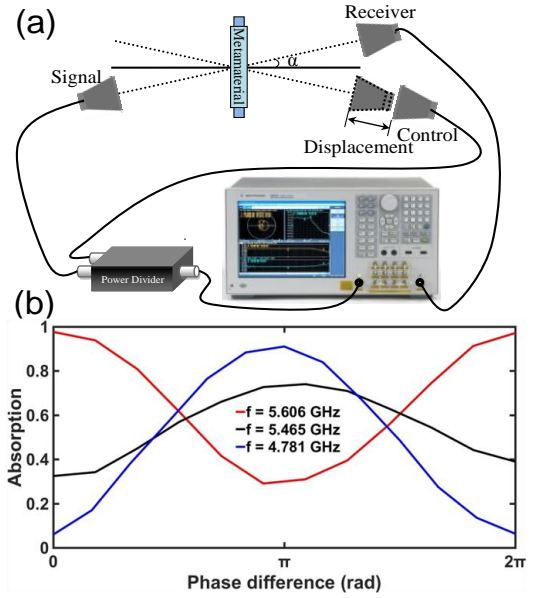


Fig. 3. (a) Schematic of experimental setup of coherent control absorption. (b) Amplitude of coherent control absorption spectra vs. phase difference of two beam for selected three frequencies of variational absorption correspond to Fig. 2(a).

The measured absorption spectra of the two bilayered metamaterials were completed at incidence in the frequency range from 4 to 8 GHz. The experiments were carried out in an anechoic chamber using broadband horn antennas and a vector network analyzer. The schematic system has been shown in Fig. 3(a). The signal from one port of vector network analyzer (model: Anritsu MS4644A) has been divided by a power divider and propagated through two antennas (model: SCHWARZBECK BBHA 9120 D) which have been placed in opposite sides of the sample. One of the senders has been selected as characterizing signal (has been labeled “signal beam”) and a receiver antenna has been placed in the opposite side of this sender, for measuring the output signal. Another sender has been labeled as “control beam”. The schematic of ideal system has been shown in Figure 2. Due to experimental limitation, it is impossible to experiment performed in the normal incident and the control beam and receiver have been

placed as close as possible to normal incident ($\alpha \sim 13^\circ$). The signal beam has been placed in the similar angle to preserve the symmetry of the system. The coherent control process should operate by changing the phase of control and signal beam in order to generate constructive and destructive interference. However, the phase difference was changed by moving the position of the control antenna by 5 mm steps, due to experimental limitations as shown in Figures 3(a). Similar to the single beam, the linear polarization transmission coefficients have been calculated for any combinations of polarization between the receiver and senders while control and signal beam had the same polarization. Figures 3(b) shows coherent absorption of the bilayered metamaterial with the phase difference varying from 0 to 2π . Evidently, two resonant absorption peaks that overlap in the single beam illumination case can be well recognized in the coherent case. The polarization-sensitive coherent perfect absorbers with high absorption have been achieved depending on the phase difference between two coherent beams. Obviously, the experimental and simulation results agree well with each other.

IV. CONCLUSIONS

In summary, we have numerically and experimentally demonstrated polarization-controlled multifrequency CPAs in microwave and optical stereometamaterials with twist ASR dimers. The electromagnetic modes in the stereometamaterials are dominated by the twist angles of the ASR dimers and can be recognized by their coherent absorption spectra. The zero and unitary absorption at each CPA can be coherently modulated by interferometric effect of two counter-propagating coherent beams. The manipulation of the operation frequencies of the CPAs has been accomplished by changing the polarization state of incident waves. The polarization state offers a freedom to design coherent perfect absorbers and the proposed scheme is beneficial to realize tunable polarization-dependent multifrequency absorbers and opens up a new opportunity for coherent spectroscopy.

ACKNOWLEDGMENT

The work is supported by Fundamental Research Funds for Harbin Engineering University (HEU) of China, National Natural Science Foundation of China (NSFC) (61675054 and 91750107), Natural Science Foundation of Heilongjiang Province (A2015014), 111 project to the Harbin Engineering University (B13015).

REFERENCES

- [1] D. Schurig, J. J. Mock, B. J. Justice, S. A. Cummer, J. B. Pendry, A. F. Starr, and D. R. Smith, "Metamaterial electromagnetic cloak at microwave frequencies," *Science*, vol. 314(5801), pp. 977-980, 2006.
- [2] N. Yu, P. Genevet, M. A. Kats, F. Aieta, J. P. Tetienne, F. Capasso, and Z. Gaburro, "Light Propagation with Phase Discontinuities: Generalized Laws of Reflection and Refraction," *Science*, vol. 334(6054), pp. 333-337, 2011.
- [3] J. Hao, Y. Yuan, L. Ran, T. Jiang, J. A. Kong, C. T. Chan, and L. Zhou, "Manipulating Electromagnetic Wave Polarizations by Anisotropic Metamaterials," *Phys. Rev. Lett.*, vol. 99(6), pp. 063908, 2007.
- [4] N. I. Landy, S. Sajuyigbe, J. J. Mock, D. R. Smith, and W. J. Padilla, "Perfect metamaterial absorber," *Phys. Rev. Lett.*, vol. 100(20), pp. 207402, 2008.
- [5] X. P. Shen, T. J. Cui, J. M. Zhao, H. F. Ma, W. X. Jiang, and H. Li, "Polarization-independent wide-angle triple-band metamaterial absorber," *Opt. Express*, vol. 19(10), pp. 9401-9407, 2011.
- [6] N. Liu, M. Mesch, T. Weiss, M. Hentschel, and H. Giessen, "Infrared Perfect Absorber and Its Application As Plasmonic Sensor," *Nano Lett.*, vol. 10(7), pp. 2342, 2010.
- [7] Y. D. Chong, L. Ge, H. Cao, and A. D. Stone, "Coherent perfect absorbers: time-reversed lasers," *Phys. Rev. Lett.*, vol. 105, pp. 053901, 2010.
- [8] W. Wan, Y. D. Chong, L. Ge, H. Noh, A. D. Stone, and H. Cao, "Time-reversed lasing and interferometric control of absorption," *Science*, vol. 331(6019), pp. 889-892, 2011.
- [9] M. Pu, Q. Feng, M. Wang, C. Hu, C. Huang, X. Ma, Z. Zhao, C. Wang, and X. Luo, "Ultrathin broadband nearly perfect absorber with symmetrical coherent illumination," *Opt. Express*, vol. 20(3), pp. 2246-2254, 2012.
- [10] J. Zhang, K. F. MacDonald, and N. I. Zheludev, "Controlling light-without light without nonlinearity," *Light: Sci. Appl.*, vol. 1, pp. e18, 2012.
- [11] Y. Fan, F. Zhang, Q. Zhao, Z. Wei, and H. Li, "Tunable terahertz coherent perfect absorption in a monolayer graphene," *Opt. Lett.*, vol. 39(21), pp. 6269-6272, 2014.
- [12] Y. Sun, W. Tan, H. Q. Li, J. Li, and H. Chen, "Experimental demonstration of a coherent perfect absorber with PT phase transition," *Phys. Rev. Lett.*, vol. 112(14), pp. 143903, 2014.
- [13] M. Kang, Y. D. Chong, H. T. Wang, W. Zhu, and M. Premaratne, "Critical route for coherent perfect absorption in a Fano resonance plasmonic system," *Appl. Phys. Lett.*, vol. 105(13), pp. 131103, 2014.
- [14] W. Tan, C. H. Zhang, C. Li, X. Y. Zhou, X. Q. Jia, Z. Feng, J. Su, and B. B. Jin, "Selective coherent perfect absorption of subradiant mode in ultrathin bi-layer metamaterials via antisymmetric excitation," *Appl. Phys. Lett.*, vol. 110(18), pp. 181111, 2017.
- [15] G. Y. Nie, Q. C. Shi, Z. Zhu, and J. H. Shi, "Selective coherent perfect absorption in metamaterials," *Appl. Phys. Lett.*, vol. 105(20), pp. 201909, 2014.
- [16] M. L. Tseng, X. Fang, V. Savinov, P. C. Wu, J.-Y. Ou, N. I. Zheludev, and D. P. Tsai, "Coherent selection of invisible high-order electromagnetic excitations," *Sci. Rep.*, vol. 7, pp. 44488, 2017.
- [17] S. A. Mousavi, E. Plum, J. H. Shi, and N. I. Zheludev, "Coherent control of optical polarization effects in metamaterials," *Sci. Rep.*, vol. 5, pp. 8977, 2015.
- [18] J. H. Shi, X. Fang, E. T. F. Rogers, E. Plum, K. F. MacDonald, and N. I. Zheludev, "Coherent control of Snell's law at metasurfaces," *Opt. Express*, vol. 22(17), pp. 21051-21060, 2014.
- [19] Z. Liu, S. Chen, H. Cheng, Z. Li, W. Liu, and J. Tian, "Interferometric control of signal light intensity by anomalous refraction with plasmonic metasurface," *Plasmonics*, vol. 11(2), pp. 353-358, 2016.
- [20] Z. Zhu, H. Liu, D. Wang, Y. X. Li, C. Y. Guan, H. Zhang, and J. H. Shi, "Coherent control of double deflected anomalous modes in ultrathin trapezoid-shaped slit metasurface," *Sci. Rep.*, vol. 6, pp. 37476, 2016.
- [21] S. Kita, K. Takata, M. Ono, K. Nozaki, E. Kuramochi, K. Takeda, and M. Notomi, "Coherent control of high efficiency metasurface beam deflectors with a back partial reflector," *APL Photonics*, vol. 2(4), pp. 046104, 2017.
- [22] M. Kang, H. Wang, and W. Zhu, "Wavefront manipulation with a dipolar metasurface under coherent control," *J. Appl. Phys.*, vol. 122(1), pp. 013105, 2017.
- [23] X. Fang, K. F. MacDonald, and N. I. Zheludev, "Controlling light with light using coherent metadevices: all-optical transistor, summator and inverter," *Light: Sci. Appl.*, vol. 4, pp. e292, 2015.
- [24] M. Papaioannou, E. Plum, J. Valente, E. Rogers, and N. I. Zheludev, "Two-dimensional control of light with light on metasurfaces," *Light: Sci. Appl.*, vol. 5(4), pp. e16070, 2016.
- [25] D. G. Baranov, A. E. Krasnok, T. Shegai, A. Alù, and Y. D. Chong, "Coherent perfect absorbers: linear control of light with light," *Nat. Rev. Mater.*, vol. 2(12), pp. 17064, 2017.

